ChemComm

COMMUNICATION

View Article Online
View Journal | View Issue

Cite this: *Chem. Commun.*, 2023, 59, 13891

Received 29th June 2023,
Accepted 24th October 2023

DOI: 10.1039/d3cc03147k

rsc.li/chemcomm

Ammonium fluoride additive-modified interphase chemistry stabilizes zinc anodes in aqueous electrolytes†

Wei Zhang, ‡[ab] Xian Wu,‡[b] Qingjin Fu,‡[b] Haotian Qu,[b] Joanna Borowiec,[a] Mark Isaacs,[a] Guangmin Zhou,[b] Ivan P. Parkin *[a] and Guanjie He *[a]

Herein, ammonium fluoride is reported as an additive within 1 M $ZnSO_4$ aqueous electrolyte to improve zinc anodes. The as-formed electrostatic shielding layer and ZnF_2-rich solid-state interphase layer can jointly inhibit side reactions and dendrite growth. Consequently, symmetric Zn‖Zn cells, asymmetric Zn‖Cu cells and Zn‖MnO_2 cells with the additives present dramatically enhanced performance in comparison to the ones with pure $ZnSO_4$ electrolyte counterparts. This work proposes a facile but effective method to achieve highly reversible zinc anodes.

As the global demand for energy storage systems soars, more reliable and more sustainable battery technologies are of great promise for building a carbon-neutral society.[1–3] Although sodium-ion batteries are emerging as a promising complementarity to the lithium-ion battery in light of the abundant Na resources and lower costs,[4,5] the common flammability issue of organic electrolytes is still hard to solve.[6] Alternatively, aqueous zinc-metal batteries have attracted much attention because of their intrinsic safety and environmental benignity.[7–9] However, the dendrite formation, water-related side reactions and formation of by-products (*e.g.*, $Zn_4(OH)_6(SO_4)\cdot 5H_2O$; Fig. 1a) impede their application, which urgently needs to be addressed.[10,11]

Numerous strategies such as zinc surface coating,[12,13] alloying,[14] textured zinc anodes,[15] and construction of 3D zinc anodes[16] have been proposed for these problems. Nevertheless, the above methods suffer from operational complexity and insufficient performance. Electrolyte engineering is deemed as an alternative and promising approach.[17–20] One pioneering work by Wang *et al.* adopted a "water-in-salt" route that involves 20 m LiTFSI and 1 m $Zn(TFSI)_2$ (m: mol kg^{-1}) to achieve a nearly 100% Coulombic efficiency.[21] But the significantly increased viscosity and cost as well as reduced ionic conductivity should not be neglected. With more available concerns, additive design in dilute electrolytes can be a better approach on account of the efficient and economic manipulation.[22,23] Our group previously reported LiCl as an electrolyte additive to efficiently regulate the plating/stripping behaviors of zinc anodes.[24] But the electrochemical properties remain to be further improved. Herein, ammonium fluoride (NF) is proposed as an additive in aqueous 1 M $ZnSO_4$ electrolyte in consideration of its characteristics of non-flammability, high solubility in water (0.835 g ml^{-1}), light weight (37.037 g mol^{-1}) and low cost (~220 USD kg^{-1}). It is found that ammonium cations are preferably adsorbed on the zinc surface to construct an electrostatic shielding layer and the dissolved fluoride anions help to build a ZnF_2-rich interphase layer, which contributes to inhibiting zinc dendrite growth, mitigating side reactions and restraining by-products, as illustrated in Fig. 1b. Benefiting from the NF additive, the Zn‖Cu cell exhibited an average Coulombic efficiency of 99.3% for 800 cycles at 1 mA cm^{-2}; besides, the Zn‖Zn cells could stably cycle for 1450 h at 1 mA cm^{-2} and 1100 h at 4 mA cm^{-2}; the Zn‖MnO_2 full cell demonstrated a much-improved cycling stability. Therefore, this low-cost inorganic additive can effectively improve the reversibility of zinc anodes for aqueous batteries.

Fig. S1 (ESI†) shows that NF additives can be totally dissolved in water. The pH values of these electrolytes are in a normal mild acidic range of 4.2–5 (Fig. S2, ESI†). Raman and Fourier-transform infrared (FT-IR) spectroscopy are initially carried out to determine if the NF additive can influence the solvation structure of Zn^{2+}. Different from other works, it turns out that no apparent deviation could be found among electrolytes with/without NF additives (Fig. S3, ESI†). One can conclude that the NF additive cannot change the solvation structure of Zn^{2+}.[25] To our knowledge, a high Coulombic efficiency (CE) of the Zn‖Cu configuration is a reliable

[a] *Christopher Ingold Laboratory, Department of Chemistry, University College London, London WC1H 0AJ, UK. E-mail: i.p.parkin@ucl.ac.uk, g.he@ucl.ac.uk*

[b] *Tsinghua Shenzhen International Graduate School, Tsinghua University, Shenzhen 518055, P. R. China*

† Electronic supplementary information (ESI) available. See DOI: https://doi.org/10.1039/d3cc03147k

‡ These authors contributed equally.

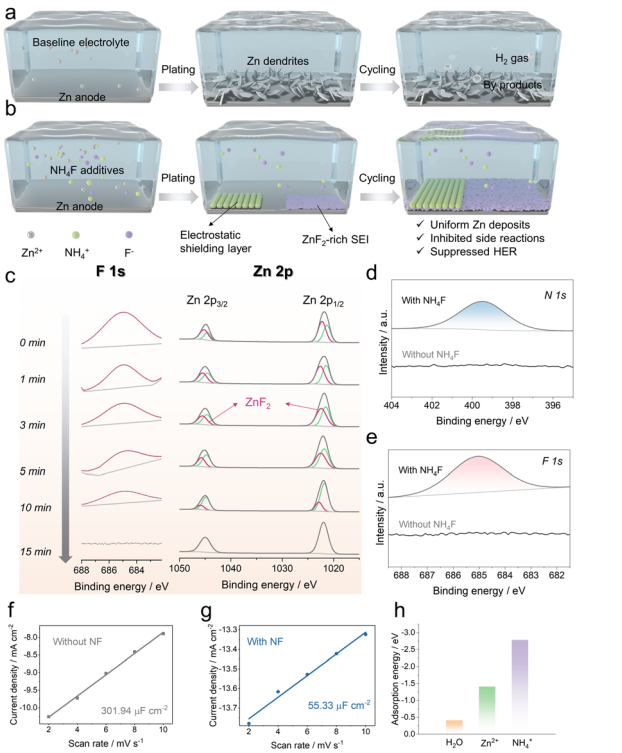

Fig. 1 Schematic illustrations of zinc anodes cycling under electrolytes (a) without NF additives and (b) with NF additives. (c) XPS depth profiles of F 1s and Zn 2p spectra of the cycled zinc electrode surface in the electrolyte with NF additives. XPS spectra of (d) N 1s and (e) F 1s of Zn foils after soaking in 25 mM NF solution and water. Linear fits to calculate EDLC values (f) without NF and (g) with NF. (h) Adsorption energy comparison of H_2O, Zn^{2+} and NH_4^+ on Zn (101).

demonstrator of high reversibility of the Zn anode.[20,22] As displayed in Fig. S4 (ESI†), the average CE of the Zn‖Cu cell with 25 mM NF is 99.3% at 1 mA cm^{-2} and 0.5 mA h cm^{-2} for 800 cycles, which is better than that of the Zn‖Cu cell with 10 mM NF (98.8%, 500 cycles) and the one with 50 mM NF (98.6%, 450 cycles) under identical conditions. Similar results can be found in Fig. S5 (ESI†) in a hybrid mode.[9] Therefore, 1 M $ZnSO_4$ + 25 mM NF (DE) is the optimal electrolyte in this work (baseline 1 M $ZnSO_4$ is denoted as BE).

To form a clearer picture on the functional mechanism of NF additives, we analyzed the surface composition of the cycled Zn foil under DE *via* Ar^+ sputtering X-ray photoelectron spectroscopy (XPS) depth profile. As seen in Fig. 1c, there has been emerging a clear peak associated with fluorine (F) on the cycled Zn surface in DE. This could be indexed to the ZnF_2 interphase from the reaction between the dissolved F^- and Zn^{2+}. With the sputtering time increasing, the ZnF_2 concentration gradually decreased and disappeared in 15 min. The thickness of the ZnF_2 SEI layer should be ~10 nm according to the previous report.[26] The electronically insulating nature (band gap: 3.46 eV) and superior mechanical properties (bulk modulus is up to 101 GPa; shear modulus is up to 39 GPa)[27] can stabilize the Zn anode.

Besides, Zn foils were soaked in the 25 mM NF solution and pure water for 7 days. It turns out that both N 1s (Fig. 1d) and F 1s (Fig. 1e) signals were found with adding NF in the XPS spectra;[28,29] while no peaks existed after soaking in pure water. Given that F^- anions interact with Zn^{2+} to form the ZnF_2 SEI layer as confirmed by the above analysis, the adsorption of F^- should be a preprocess before SEI formation. The reduced electric double-layer capacitance (EDLC) value in Fig. 1g compared with the baseline in Fig. 1f supports the adsorption of NF additives on the Zn surface. Fig. 1h shows a much more negative adsorption energy of NH_4^+ than those of H_2O and Zn^{2+} on the Zn surface. These results show that NH_4^+ was adsorbed on the surface of the Zn anodes and thus a "shielding effect" can be formed, water can be excluded, and uniform Zn deposition can be achieved (Fig. 1b).

Then, *in situ* optical microscopy and scanning electron microscopy (SEM) were performed to investigate the morphologies of the cycled Zn anodes in different electrolytes. In Fig. 2a and c, the deposited Zn exhibited quasi-hexagonal platelet shapes and Zn dendrites after cycling in BE, in line with previous aqueous $ZnSO_4$ research.[23,30] In sharp contrast, as shown in Fig. 2b and d, the Zn deposits exhibit dense and smooth morphologies with the NF additive (DE).

The influence of the NF additive on the Zn anode corrosion resistance was quantified by linear polarization measurements (Fig. 2e). The corrosion current density of the Zn anode is decreased with the assistance of the NF additive (15.6 μA cm^{-2}) from the baseline case (BE, 57.6 μA cm^{-2}), which demonstrates improved corrosion resistance of the Zn anodes in DE. The

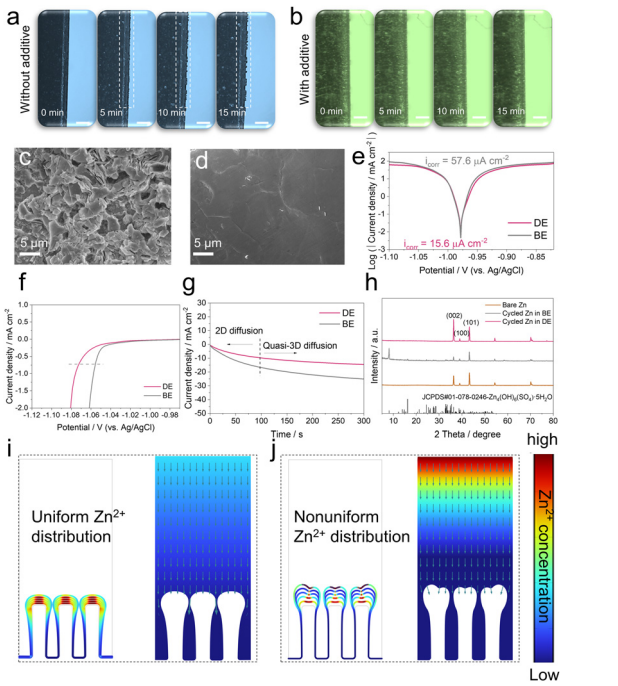

Fig. 2 *In situ* optical microscopy images of Zn‖Zn cells at 10 mA cm^{-2} in (a) BE and (b) DE (scale bar: 300 μm). SEM images of cycled zinc foils in (c) BE and (d) DE. (e) Linear polarization curves of zinc anodes. (f) HER performances. (g) CA curves of Zn plates at −150 mV. (h) XRD patterns of the bare Zn and cycled Zn. COMSOL simulation results of the zinc concentrations of the (i) DE system and (j) BE system.

good corrosion suppression effect was also verified by the hydrogen evolution reaction (HER) results in different electrolytes through liner sweep voltammetry (LSV). In Fig. 2f, the NF additive leads to a more negative reduction potential than the baseline, indicative of better HER suppression.

In addition, chronoamperometry (CA, Fig. 2g) is a common method to characterize the Zn nucleation and growth. To our knowledge, a higher current density response represents an increased effective surface area.[22,25] When subjected to an overpotential of −150 mV, there is a rapid current density response for both samples at the initial stages, corresponding to the Zn nucleation. As this process continues, the Zn‖Zn cell using BE still exhibited increased current density responses, demonstrative of a larger effective area and thereby the Zn dendrites could be formed. By contrast, a lower increase in current density response could be found with the introduction of the NF additive. This accords to a smoother and denser Zn electrodeposition in Fig. 1b, 2b and 2d.

Furthermore, we collected XRD patterns of Zn foils after cycling in BE and DE as well as the bare Zn foil. As shown in Fig. 2h, intense impurity peaks of $Zn_4(OH)_6(SO_4)\cdot 5H_2O$ (ZHS, JCPDS#01-078-0246) can be found in the cycled Zn in BE. According to previous works, the ZHS by-product usually has high specific surface areas, which leads to a non-uniform zinc deposit and consumes a plethora of Zn^{2+} and deteriorates dendrite growth. However, no ZHS peaks can be observed, indicative of the positive effect of the NF additive. Of note, Zn(002) becomes the dominant crystal plane after adding the NF. The (002) surface usually displays better anti-corrosion and dendrite inhibition behaviors than the (101) and (100) planes.[22,31,32] The above analyses confirm that the NF additive is favorable for inhibiting water-related side reactions and by-product formation as well as suppressing dendrite growth. COMSOL Multiphysics simulation was further conducted. As seen in Fig. 2i, j and Fig. S7 (ESI†), with NF additives, Zn^{2+} concentration and electric field distribution around the Zn anode and deposition morphologies became much smoother as a result of the modified interface by NF additives.

Additionally, 12.5 mM ZnF_2 and 12.5 mM $(NH_4)_2SO_4$ were respectively introduced into 1 M $ZnSO_4$ to investigate the separate functions of F^- and NH_4^+ on battery performance. In Fig. 3a and b, it can be found that the Zn‖Cu cell with ZnF_2 presents an enhanced average CE of 98.7% at 1 mA cm^{-2} (98.2% for the one with $(NH_4)_2SO_4$) while the baseline only achieves a low average CE (95.1%) within 100 cycles. With regard to the Zn‖Zn symmetric cell cases subjected to 4 mA cm^{-2} with a capacity of 0.5 mA cm^{-2}, both cells demonstrate longer lifespans and higher stabilities (935 h for the ZnF_2 cell and 600 h for the $(NH_4)_2SO_4$ cell) but the baseline fails within 250 h. The above results confirm the acceptable but not good enough positive effects of F^- and NH_4^+ on the stripping/plating behaviors of Zn anodes.

To present synergistic functions of F^- and NH_4^+ on Zn plating/stripping behaviors, various battery configurations were tested. From Fig. 4a and b, the Zn‖Cu cell with NF presents a higher average CE of 99.3% within 800 cycles at 1 mA cm^{-2} and

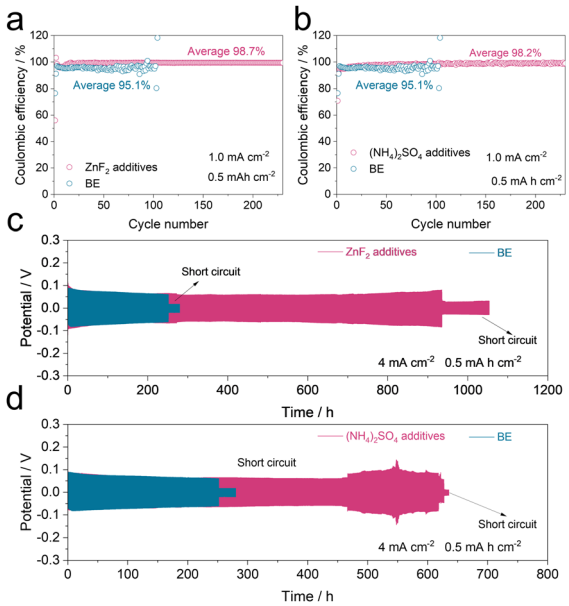

Fig. 3 Coulombic efficiencies of Zn‖Cu cells at 1 mA cm^{-2} in 1 M $ZnSO_4$ and the designed electrolyte with (a) 12.5 mM ZnF_2 and (b) 12.5 mM $(NH_4)_2SO_4$. Cycling properties of Zn‖Zn symmetric cells at 4 mA cm^{-2} and 0.5 mA h cm^{-2} in 1 M $ZnSO_4$ and the designed electrolyte with (c) 12.5 mM ZnF_2 and (d) 12.5 mM $(NH_4)_2SO_4$.

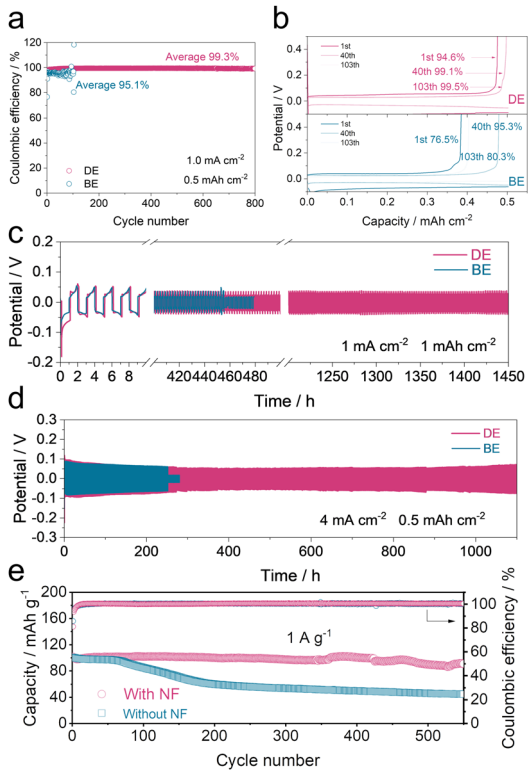

Fig. 4 (a) Coulombic efficiencies of Zn‖Cu cells at 1 mA cm^{-2} and corresponding (b) charge/discharge curves. Cycling performances of Zn‖Zn cells at (c) 1 mA cm^{-2} and 1 mA h cm^{-2}, and (d) 4 mA cm^{-2} and 0.5 mA h cm^{-2}. (e) Cycling capabilities of Zn‖MnO_2 cells at 1 A g^{-1}.

0.5 mA h cm^{-2} than the baseline (95.1%, 100 cycles) as well as a higher initial CE (94.6% *vs.* 76.5%). Secondly, the Zn‖Zn symmetric cells with NF display apparently boosted lifespans compared to the baseline cells (1450 h *vs.* 450 h at 1 mA cm^{-2} and 1 mA h cm^{-2}, Fig. 4c; 1100 h *vs.* 250 h at 4 mA cm^{-2} and 0.5 mA h cm^{-2}, Fig. 4d; 460 h *vs.* 84 h at 10 mA cm^{-2} and 1 mA h cm^{-2}, Fig. S8, ESI†). These performances outweigh many previous reports as seen in Table S1 (ESI†). Finally, with more practical concerns, the Zn‖MnO_2 full cell with the presence of the NF additive displays a much-improved cycling stability at 1 A g^{-1} (Fig. 4e).

In summary, we studied NF as an additive in 1 M aqueous $ZnSO_4$ electrolyte. An electrostatic shielding layer from NH_4^+ cations and a ZnF_2-rich SEI layer from the dissolved F^- anions were constructed; thereby zinc dendrites, water-related side reactions and by-products can be suppressed. The NF additive contributed to improved battery performance: (i) the Zn‖Cu cell presented an average CE of 99.3% throughout 800 cycles at 1 mA cm^{-2}; (ii) the Zn‖Zn symmetric cells are capable of stably running for 1450 h at 1 mA cm^{-2} and 1100 h at 4 mA cm^{-2}; (iii) the Zn‖MnO_2 full cell displayed boosted cycling stability at 1 A g^{-1}. Hence, this work proposes an applicable and efficient approach for boosting the reversibility of aqueous Zn batteries.

W. Zhang thanks the funding support from the China Scholarship Council/University College London for the joint PhD scholarship. The authors would like to acknowledge the Engineering and Physical Sciences Research Council (EPSRC, EP/V027433/3), the Royal Society (RGS\R1\211080; IEC\NSFC\201261), UK Research and Innovation (UKRI) under the UK government's Horizon Europe funding guarantee (101077226; EP/Y008707/1), and the STFC Batteries Network (ST/R006873/1). The authors also thank HarwellXPS for assisting with the XPS analysis and Dr Zhenming Xu for the DFT calculations.

Conflicts of interest

There are no conflicts to declare.

Notes and references

1 Z. Zhu, T. Jiang, M. Ali, Y. Meng, Y. Jin, Y. Cui and W. Chen, *Chem. Rev.*, 2022, **122**, 16610–16751.
2 T. Wang, Y. Jin, T. Mu, T. Wang and J. Yang, *J. Membr. Sci.*, 2022, **654**, 120539.
3 R. Chen, H. Tang, P. He, W. Zhang, Y. Dai, W. Zong, F. Guo, G. He and X. Wang, *Adv. Funct. Mater.*, 2023, **33**, 2212078.
4 W. Zhang, Y. Wu, Z. Xu, H. Li, M. Xu, J. Li, Y. Dai, W. Zong, R. Chen, L. He, Z. Zhang, D. J. L. Brett, G. He, Y. Lai and I. P. Parkin, *Adv. Energy Mater.*, 2022, **12**, 2201065.
5 W. Zhang, Y. Wu, Y. Dai, Z. Xu, L. He, Z. Li, S. Li, R. Chen, X. Gao, W. Zong, F. Guo, J. Zhu, H. Dong, J. Li, C. Ye, S. Li, F. Wu, Z. Zhang, G. He, Y. Lai and I. P. Parkin, *Chem. Sci.*, 2023, **14**, 8662–8671.
6 L. E. Blanc, D. Kundu and L. F. Nazar, *Joule*, 2020, **4**, 771–799.
7 R. Chen, C. Zhang, J. Li, Z. Du, F. Guo, W. Zhang, Y. Dai, W. Zong, X. Gao, J. Zhu, Y. Zhao, X. Wang and G. He, *Energy Environ. Sci.*, 2023, **16**, 2540–2549.
8 Y. Dai, C. Zhang, W. Zhang, L. Cui, C. Ye, X. Hong, J. Li, R. Chen, W. Zong, X. Gao, J. Zhu, P. Jiang, Q. An, D. J. L. Brett, I. P. Parkin, G. He and L. Mai, *Angew. Chem., Int. Ed.*, 2023, **62**, e202301192.
9 X. Yu, Z. Li, X. Wu, H. Zhang, Q. Zhao, H. Liang, H. Wang, D. Chao, F. Wang, Y. Qiao, H. Zhou and S.-G. Sun, *Joule*, 2023, **7**, 1145–1175.
10 Y. Zhang, H. Dong, T. Wang, G. He, I. P. Parkin and F. Cegla, *J. Power Sources*, 2022, **542**, 231730.
11 X. Gao, Y. Dai, C. Zhang, Y. Zhang, W. Zong, W. Zhang, R. Chen, J. Zhu, X. Hu, M. Wang, R. Chen, Z. Du, F. Guo, H. Dong, Y. Liu, H. He, S. Zhao, F. Zhao, J. Li, I. P. Parkin, C. J. Carmalt and G. He, *Angew. Chem., Int. Ed.*, 2023, **62**, e202300608.
12 H. Dong, X. Hu, R. Liu, M. Ouyang, H. He, T. Wang, X. Gao, Y. Dai, W. Zhang, Y. Liu, Y. Zhou, D. J. L. Brett, I. Parkin, P. Shearing and G. He, *Angew. Chem., Int. Ed.*, 2023, e202311268, DOI: **10.1002/anie.202311268**.
13 Z. Zhao, R. Wang, C. Peng, W. Chen, T. Wu, B. Hu, W. Weng, Y. Yao, J. Zeng, Z. Chen, P. Liu, Y. Liu, G. Li, J. Guo, H. Lu and Z. Guo, *Nat. Commun.*, 2021, **12**, 6606.
14 H. Tian, Z. Li, G. Feng, Z. Yang, D. Fox, M. Wang, H. Zhou, L. Zhai, A. Kushima, Y. Du, Z. Feng, X. Shan and Y. Yang, *Nat. Commun.*, 2021, **12**, 237.
15 J. Zheng, Q. Zhao, T. Tang, J. Yin, C. D. Quilty, G. D. Renderos, X. Liu, Y. Deng, L. Wang, D. C. Bock, C. Jaye, D. Zhang, E. S. Takeuchi, K. J. Takeuchi, A. C. Marschilok and A. L. Archer, *Science*, 2019, **366**, 645–648.
16 N. Guo, W. Huo, X. Dong, Z. Sun, Y. Lu, X. Wu, L. Dai, L. Wang, H. Lin, H. Liu, H. Liang, Z. He and Q. Zhang, *Small Methods*, 2022, **6**, 2200597.
17 W. Zhang, Y. Dai, R. Chen, Z. Xu, J. Li, W. Zong, H. Li, Z. Li, Z. Zhang, J. Zhu, F. Guo, X. Gao, Z. Du, J. Chen, T. Wang, G. He and I. Parkin, *Angew. Chem., Int. Ed.*, 2023, **62**, e202212695.
18 W. Zhang and G. He, *Angew. Chem., Int. Ed.*, 2023, **62**, e202218466.
19 R. Chen, W. Zhang, Q. Huang, C. Guan, W. Zong, Y. Dai, Z. Du, Z. Zhang, J. Li, F. Guo, X. Gao, H. Dong, J. Zhu, X. Wang and G. He, *Nano-Micro Lett.*, 2023, **15**, 81.
20 L. Cao, D. Li, T. Pollard, T. Deng, B. Zhang, C. Yang, L. Chen, J. Vatamanu, E. Hu, M. J. Hourwitz, L. Ma, M. Ding, Q. Li, S. Hou, K. Gaskell, J. T. Fourkas, X. Q. Yang, K. Xu, O. Borodin and C. Wang, *Nat. Nanotechnol.*, 2021, **16**, 902–910.
21 F. Wang, O. Borodin, T. Gao, X. Fan, W. Sun, F. Han, A. Faraone, J. A. Dura, K. Xu and C. Wang, *Nat. Mater.*, 2018, **17**, 543–549.
22 R. Zhao, H. Wang, H. Du, Y. Yang, Z. Gao, L. Qie and Y. Huang, *Nat. Commun.*, 2022, **13**, 3252.
23 Z. Hu, F. Zhang, Y. Zhao, H. Wang, Y. Huang, F. Wu, R. Chen and L. Li, *Adv. Mater.*, 2022, **34**, 2203104.
24 X. Guo, Z. Zhang, J. Li, N. Luo, G.-L. Chai, T. S. Miller, F. Lai, P. Shearing, D. J. L. Brett, D. Han, Z. Weng, G. He and I. P. Parkin, *ACS Energy Lett.*, 2021, **6**, 395–403.
25 C. Huang, X. Zhao, S. Liu, Y. Hao, Q. Tang, A. Hu, Z. Liu and X. Chen, *Adv. Mater.*, 2021, **33**, 2100445.
26 C. Li, A. Shyamsunder, A. G. Hoane, D. M. Long, C. Y. Kwok, P. G. Kotula, K. R. Zavadil, A. A. Gewirth and L. F. Nazar, *Joule*, 2022, **6**, 1103–1120.
27 A. Jain, S. P. Ong, G. Hautier, W. Chen, W. D. Richards, S. Dacek, S. Cholia, D. Gunter, D. Skinner, G. Ceder and K. A. Persson, *APL Mater.*, 2013, **1**, 011002.
28 R. Guo, X. Liu, X. Zhang, W. Wei, G. Li, X. Yin, C. Zhang, Y. Zhao, Q. Guo, S. He, C. Xu and B. Shen, *Catal. Today*, 2022, **402**, 104–114.
29 D. Chadwick and T. Hashemi, *Corros. Sci.*, 1978, **18**, 39–51.
30 H. Qin, W. Kuang, N. Hu, X. Zhong, D. Huang, F. Shen, Z. Wei, Y. Huang, J. Xu and H. He, *Adv. Funct. Mater.*, 2022, **32**, 2206695.
31 D. Yuan, J. Zhao, H. Ren, Y. Chen, R. Chua, E. T. J. Jie, Y. Cai, E. Edison, W. Manalastas, Jr., M. W. Wong and M. Srinivasan, *Angew. Chem., Int. Ed.*, 2021, **60**, 7213–7219.
32 M. Zhou, S. Guo, J. Li, X. Luo, Z. Liu, T. Zhang, X. Cao, M. Long, B. Lu, A. Pan, G. Fang, J. Zhou and S. Liang, *Adv. Mater.*, 2021, **33**, 2100187.

